

Characterizing entanglement in qubits created with spatially correlated twin photons

Leonardo Neves,^{1,2,*} G. Lima,^{2,3} E. J. S. Fonseca,⁴ L. Davidovich,⁵ and S. Pádua²

¹Clarendon Laboratory, Oxford University, Parks Road, Oxford, OX1 3PU, United Kingdom

²Departamento de Física, Universidade Federal de Minas Gerais, Caixa Postal 702, Belo Horizonte, MG 30123-970, Brazil

³Group of Applied Physics, University of Geneva, 1211 Geneva 4, Switzerland

⁴Instituto de Física, Universidade Federal de Alagoas, Cidade Universitária, Maceió, AL 57072-970, Brazil

⁵Instituto de Física, Universidade Federal do Rio de Janeiro, Caixa Postal 68528, 21941-972, Rio de Janeiro, RJ, Brazil

(Received 8 June 2007; published 12 September 2007)

We characterize entanglement in two-qubit pure states encoded in transverse momenta of twin photons obtained from spontaneous parametric down-conversion. Two alternate methods are employed: (i) measurement of conditional interference patterns and (ii) measurement of the marginal probability that yields the single-photon interference pattern. Both methods are local with classical communication and rely on Schmidt decomposition of the quantum state, which is generated by letting the photons propagate through an appropriate lens system. In both cases we can obtain the concurrence either through the Schmidt coefficients in the first method or directly relating the concurrence to the visibility of the interference pattern in the second one.

DOI: 10.1103/PhysRevA.76.032314

PACS number(s): 03.67.Mn, 03.65.-w

I. INTRODUCTION

Entanglement is not only an essential trait of quantum mechanics, but also a basic ingredient in quantum information [1]. Its characterization is therefore important for practical and conceptual reasons. While this is still an open problem for multipartite systems, measures for bipartite entanglement, like the concurrence introduced by Wootters [2], are based on mathematical operations that do not have an operational counterpart and require a tomographic reconstruction of the quantum state [3,4]. Finding physical ways of characterizing entanglement, without the need for a full reconstruction of the state, is thus an attractive goal, with both basic and practical motivations. For *pure* states of bipartite two-level quantum systems (qubits), this problem becomes simpler, since then a single parameter characterizes simultaneously the degree of entanglement and the degree of mixing of the reduced density matrix of either subsystem. Based on this fact, two recent works show that for N copies of the two-qubit pure state, global and local coherent measurements (joint measurement in N copies) [5] and local incoherent ones (measurements on one copy at a time) [6] are optimal for estimating entanglement. Direct detection of entanglement for two-qubit polarization pure states, generated by spontaneous parametric down-conversion (SPDC), was demonstrated in [7], with only two copies of the state, realized on the polarization and momentum degrees of freedom.

For entangled polarizations, robust techniques for characterizing entanglement have been proposed [4]. In this work, we present experimental methods for characterizing entanglement in two-qubit pure states encoded in transverse momentum of twin photons from SPDC. This kind of entangled states has been recently demonstrated for qubits [8,9], but there their entanglement was characterized only qualitatively, and we also restrict ourselves to maximally entangled states. Here, we show that by manipulating the pump

beam we can prepare states with different degrees of entanglement which will be characterized quantitatively in two ways: (i) by measuring the two-photon conditional interference and (ii) by measuring marginal interference patterns. As we will see, both strategies are local with classical communication and both rely on Schmidt decomposition. The degree of entanglement will be then quantified by concurrence in both cases.

A general pure state of two qubits can be expanded in the basis $\{|0\rangle, |1\rangle\} \otimes \{|0\rangle, |1\rangle\}$ as

$$|\psi\rangle = c_{11}|11\rangle + c_{10}|10\rangle + c_{01}|01\rangle + c_{00}|00\rangle. \quad (1)$$

The concurrence which quantifies entanglement in this system is given by [2]

$$\mathcal{C}(\psi) = 2|c_{11}c_{00} - c_{10}c_{01}|. \quad (2)$$

It is equal to 0 for a product state and to 1 for a maximally entangled state. The Schmidt decomposition consists in find another basis ($\{|a\rangle, |a'\rangle\}$) for each subsystem such that we can write the state (1) as [10]

$$|\psi\rangle = c_a|aa\rangle + c_{a'}|a'a'\rangle, \quad (3)$$

where $\{|a\rangle, |a'\rangle\}$, is the *Schmidt basis* and the Schmidt coefficients c_a and $c_{a'}$ are real and positive. In terms of these coefficients, the concurrence is given by the simpler expression

$$\mathcal{C}(\psi) = 2c_a c_{a'}. \quad (4)$$

Our strategy consists in making measurements in the Schmidt basis, either by directly measuring the Schmidt coefficients or through a direct connection between concurrence, given by Eq. (4), and the visibility of interference patterns. The Schmidt basis is generated by letting the photons propagate through an appropriate lens system. This strategy, besides leading to a simple determination of concurrence, yields a physical reality to the Schmidt basis in this case.

*l.neves1@physics.ox.ac.uk

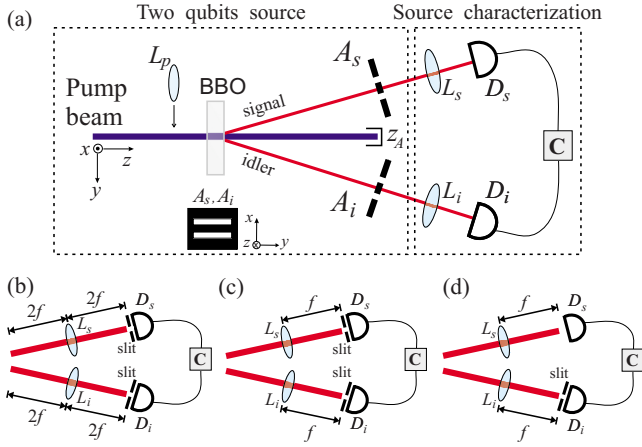


FIG. 1. (Color online) (a) Outline of the experimental setup used to create and characterize two-qubit states. (b)–(d) Configurations for characterizing the source: (b) measurement in the basis $\{|\pm\rangle_s \otimes |\pm\rangle_i\}$, (c) measurement in the Schmidt bases, and (d) measurement of marginal probability. Details in the text.

This paper is organized as follows. In Sec. II we give a brief description of the method of generating spatially entangled qubits with different degrees of entanglement by using twin photons from SPDC. In Sec. III we describe the experiment, showing the preparation and the characterization of entanglement in these two-qubit states. The results obtained are discussed. Section IV contains the conclusions.

II. THEORETICAL BACKGROUND

Let us begin by considering the SPDC process in the monochromatic, paraxial, and thin crystal approximations [11]. Under these conditions, the two-photon state corresponding to frequency-degenerated twin photons transmitted through an array of multislit (an opaque screen with D transparent slits of width $2a$ and period d) was obtained in [8]. For $D=2$ (double slits), with the configuration shown in Fig. 1(a), it is given by

$$|\Psi\rangle = W_+ |+\rangle_s |+\rangle_i + W_0 |+\rangle_s |-\rangle_i + W_0 |-\rangle_s |+\rangle_i + W_- |-\rangle_s |-\rangle_i, \quad (5)$$

where

$$|\pm\rangle \equiv \sqrt{a/\pi} \int dq e^{\mp i q d/2} \text{sinc}(qa) |1q\rangle, \quad (6)$$

with $|1q\rangle$ denoting the one-photon state with transverse component of the wave vector equal to q [8]. The set $\{|\pm\rangle\}$ forms an orthonormal basis in the two-dimensional Hilbert space of each photon, defining the logical qubits in terms of the slit where the photon has passed through [8,9]. Referring to Fig. 1(a), states $|+\rangle$ ($|-\rangle$) correspond to the photon passing through the upper (lower) slit. The coefficients are given by $W_0 \equiv \gamma W(0; z_A) e^{i k d^2 / 8 z_A}$ and $W_{\pm} \equiv \gamma W(\pm d/2; z_A)$, where γ is a normalization constant, and $W(0; z_A)$ and $W(\pm d/2; z_A)$ are the pump-field transverse profiles at the double-slit plane (z_A) at the transverse positions $x=0$ (center of the double slit)

and $x = \pm d/2$ (center of the slits “ \pm ”), respectively. The extra phase in W_0 comes from the two photons passing one through the upper and the other through the lower slit, where k is the wave number of the pump photon. We see then that the degree of entanglement of Eq. (5) is controlled by manipulating the pump-field transverse profile, whose amplitude will be assumed symmetrical around the double-slit center—i.e., $|W_+| = |W_-|$.

As we discussed before, the two-photon state in Eq. (5) may also be written in terms of the Schmidt decomposition [10] as

$$|\Psi\rangle = c_+ |\eta_+\rangle_s |\eta_+\rangle_i + c_- |\eta_-\rangle_s |\eta_-\rangle_i, \quad (7)$$

where

$$c_{\pm} = \sqrt{1/2 \pm |W_+ W_0^* + W_0 W_-^*|} \quad (8)$$

are the Schmidt coefficients and the sets $\{|\eta_{\pm}\rangle_s\}$ and $\{|\eta_{\pm}\rangle_i\}$ are other orthonormal bases in the Hilbert space of signal and idler photons, respectively, that form the Schmidt bases for $|\Psi\rangle$. The vectors $|\eta_{\pm}\rangle$ are given by

$$|\eta_{\pm}\rangle = 1/\sqrt{2} (|+\rangle \pm e^{i\xi} |-\rangle), \quad (9)$$

where $e^{i\xi} = |W_+ W_0^* + W_0 W_-^*| / (W_+ W_0^* + W_0 W_-^*)$ is phase dependent on the pump-beam profile as well as on the external phases which can be put in the photons paths. After taking the partial trace of $|\Psi\rangle\langle\Psi|$ over either of the two subsystems, the resulting reduced density matrix is

$$\rho = c_+^2 |\eta_+\rangle\langle\eta_+| + c_-^2 |\eta_-\rangle\langle\eta_-|. \quad (10)$$

Since $c_+^2 + c_-^2 = 1$, with $c_+^2 \in [\frac{1}{2}, 1]$ and $c_-^2 \in [0, \frac{1}{2}]$, we can choose c_- as the only parameter that characterizes entanglement in our system. If $c_- = 0$, the overall state $|\Psi\rangle$ in Eq. (7) will be factorizable and the reduced density matrix in Eq. (10) will be pure; otherwise, $|\Psi\rangle$ is entangled and ρ is a statistical mixture. In particular, for $c_- = 1/\sqrt{2}$, $|\Psi\rangle$ is a maximally entangled state and ρ is a maximally mixed state. As mentioned before, the amount of entanglement present in $|\Psi\rangle$ can be determined by the concurrence [2], which is given in terms of the Schmidt coefficients in Eq. (8) by

$$\mathcal{C}(\Psi) = 2c_+ c_-. \quad (11)$$

Thus, determination of these coefficients quantifies entanglement of the spatially entangled photonic qubits.

III. EXPERIMENT

The experimental setup is sketched in Fig. 1(a). The source of qubits is in the dashed box on the left-hand side. It is composed by a 5-mm-long β -barium borate (BBO) nonlinear crystal, cut for noncollinear type-II phase matching and pumped by a 200-mW krypton laser operating at $\lambda = 413$ nm. Down-converted photons with a degenerate wavelength of 826 nm are produced at an angle of 2.5° off the pump direction, and they are sent to two double slits placed at the same distance $z_A = 200$ mm from the crystal. The slit width is $2a = 0.09$ mm, and the separation (center-to-center) between them is $d = 0.21$ mm. The twin-photon states gener-

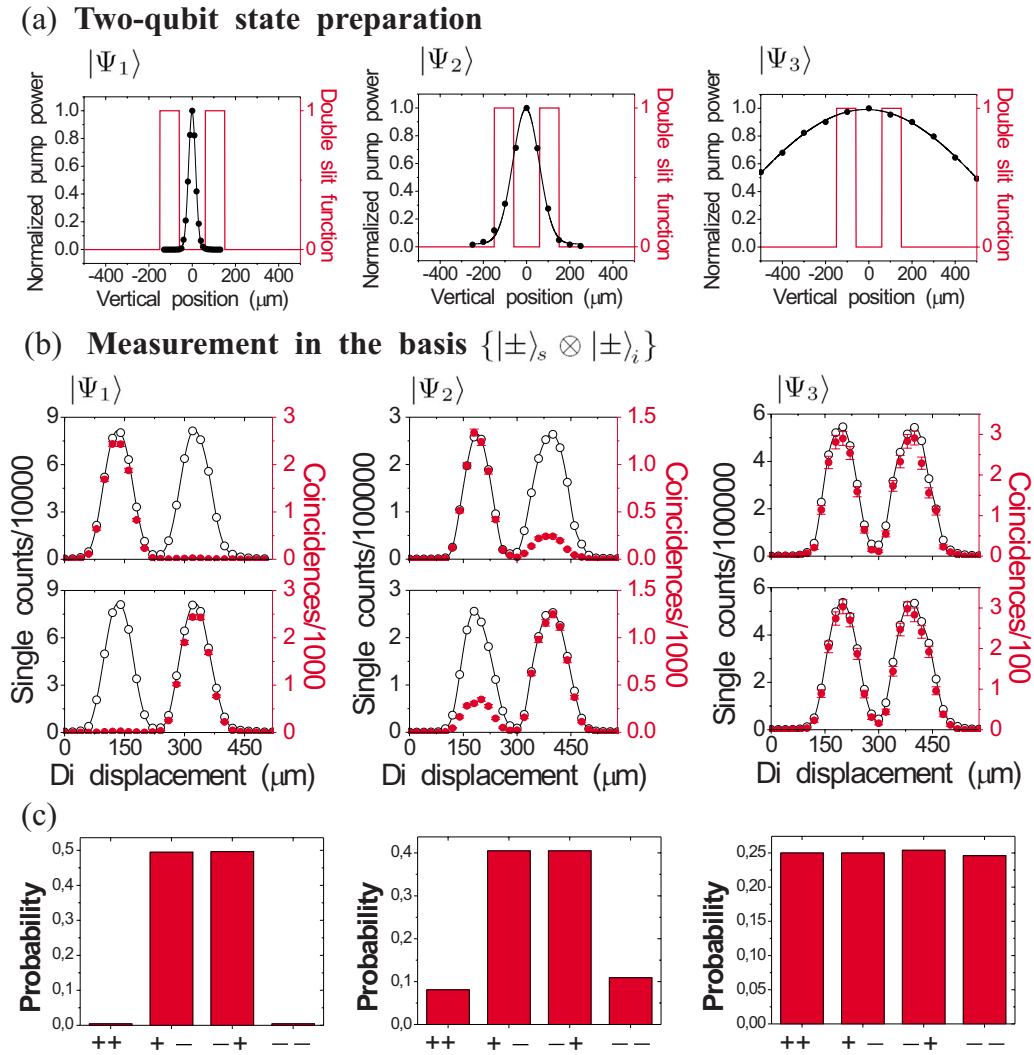


FIG. 2. (Color online) (a) Normalized pump intensity profiles used for preparing the states $|\Psi_1\rangle$, $|\Psi_2\rangle$, and $|\Psi_3\rangle$. (b) Measurements in the basis $\{|\pm\rangle_s \otimes |\pm\rangle_i\}$. D_i single counts (open circles) and D_s - D_i coincidence counts (solid circles) measured with D_s fixed at the image of slit “+” (“-”) and D_i scanning the image of idler double slit. (c) Histograms of probabilities for all basis states.

ated by this setup have a high degree of purity, higher than 99%. This has been shown in a recently developed method of quantum-state tomography for these states described in Ref. [12], which allow us to consider them to be essentially pure. The dashed box on the right-hand side shows a general scheme for characterizing the source. The transmitted twin photons are collected by convergent lenses L_s and L_i , both with focal length $f=150$ mm and fixed at a distance z_L from the crystal, and then they propagate freely toward the detectors D_s and D_i which are kept fixed at a distance $z=800$ mm from the crystal. In front of each detector there is a 0.1-mm-width single slit oriented parallel to the double slit [except in the configuration of Fig. 1(d), where the signal detector is wide open] followed by an interference filter of 8 nm bandwidth centered at 826 nm and a microscope objective focusing on their active area. The output pulses are sent to counters C , which register single and coincidence counts, with a resolving time of 5 ns.

A. State preparation

We have prepared three types of two-qubit states, denoted by $|\Psi_1\rangle$, $|\Psi_2\rangle$, and $|\Psi_3\rangle$, using only a Gaussian pump beam, for which $W_+=W_-$ in Eq. (5) and $e^{i\xi}=1$ in Eq. (9). To prepare $|\Psi_1\rangle$, a lens L_P of focal length $f=250$ mm is inserted into the pump-beam path 50 mm before the crystal [Fig. 1(a)] such that the pump is focused at the double-slit plane. For $|\Psi_2\rangle$ a lens L_P with $f=300$ mm placed 50 mm before the crystal focuses the pump beam partially at z_A . For $|\Psi_3\rangle$ there is no lens at the pump beam so that its profile at z_A will have its own laser beam width at that point. Figure 2(a) shows the normalized pump intensity profiles at the double-slit plane.

B. Measurement in the basis $\{|\pm\rangle_s \otimes |\pm\rangle_i\}$

Let us first consider measurements in the basis $\{|\pm\rangle_s \otimes |\pm\rangle_i\}$ using the setup shown in Fig. 1(b). The double slits in the signal and idler paths are imaged by the lenses L_s and

L_i on the plane of the detectors D_s and D_i , respectively, with a magnification factor of 1. Thus, the propagated state is the same as the one after the slits [13]. Coincidence measurements select the four basis states in the following way: D_i scans the image of the idler double slit in the x direction, while D_s is kept fixed at the image of slit “+” (or “−”) of the signal double slit. Each such measurement selects two of the four basis states. The experimental results for $|\Psi_1\rangle$, $|\Psi_2\rangle$, and $|\Psi_3\rangle$ are shown in Fig. 2(b). The normalized coincidence counts obtained from the four measured coincidence numbers give the probabilities [14] for each basis state [Fig. 2(c)]. We see that the correlations between the twin photons are in accordance with the pump profiles. One should note, however, these results cannot be used for characterizing *entanglement* since we have not obtained the phases of the coefficients W_0 and W_{\pm} . Indeed, just looking for these correlations we would say that $|\Psi_3\rangle$ is an uncorrelated state and we will see later that this is not the case here. This results from the fact that for two-qubit pure states it is not possible to quantify entanglement by measuring a single observable of the composite system [6], in this case the set of orthogonal projectors $|l\rangle\rangle\langle l'|$ ($l, l' = \pm$) with $\sum_{l'} |l\rangle\rangle\langle l'| = \mathbb{I}$.

C. Measurement in the Schmidt bases

In the second step, we are going to characterize entanglement in these states. As we saw, the Schmidt decomposition can be very useful for doing this. The question that arises is how to measure in the basis $\{|\eta_{\pm}\rangle\}$. The measurements in the basis $\{|\pm\rangle\}$ are done with the detector in the image plane (near field), as described in the previous section, where the fixed pointlike signal detector selects either the mode $|+\rangle$ or the mode $|-\rangle$ while the scanning pointlike idler detector measures the distribution of the respective idler mode [Fig. 2(b)]. Now, what happens if we move the detectors from the near field to the far field (Fourier transform plane)? Far from the image plane the pointlike detector selects a state which is a given superposition of $|\pm\rangle$, due to diffraction interference. Each particular superposition depends on the transverse position of the detector [12], and each one will have a specific detection probability distribution. If we measure two such distributions associated with two orthogonal states, we obtain the weights of the photon state in this new basis in the same sense we did for the basis $\{|\pm\rangle\}$. Let us check these distributions for the Schmidt modes $|\eta_{\pm}\rangle$. First, we define $\mathbb{E} \equiv \hat{E}^{(+)}(x, z)$ where $\hat{E}^{(+)}(x, z)$ is the positive-frequency part of the electric field operator and x is the detection position in the plane z . Using the methods of Fourier optics [15], the paraxial field operator for an imaging system, as shown in Fig. 1(a), can be shown to be given by [16]

$$\mathbb{E} \propto \int \int dq dq' \hat{a}(q') \exp\{i[qx - q^2(z - z_L)/2k - q'^2 \times (z_L - z_A)/2k + (q - q')^2 f/2k]\}, \quad (12)$$

which describes a free-space electric field propagating from the double-slit plane (z_A), transmitted by a thin convergent lens (with focal length f) in the plane z_L and propagating to the detector plane z . Here $\hat{a}(q')$ is the annihilation operator

of a photon with transverse wave vector q' . It is easy to check that with the detector in the focal plane of the lens—i.e., $z - z_L = f$ —the positive-frequency part of the electric field operator (up to a phase factor) in this plane will be given by

$$\mathbb{E} \propto \hat{a}(kx/2f), \quad (13)$$

which simply states a well-known fact that a lens maps transverse momenta to transverse positions ($q \rightarrow kx/f$) in its focal plane, doing in this way the Fourier transform of a given input beam [15]. Using the states $|\pm\rangle$ defined in Eq. (6), the detection probability for single photons $|\eta_{\pm}\rangle$ (with $e^{i\xi} = 1$, since we are using Gaussian beams) will be

$$P_{\eta_{\pm}}(x) \propto S^2(x)[1 \pm \cos(\alpha x)], \quad (14)$$

where $\alpha = kd/2f$ and $S(x)$ is a diffraction term given by $S(x) \equiv \text{sinc}(kax/2f)$. These distributions are shown in Fig. 3(a), where we can see typical Young’s interference patterns composed either by fringes ($|\eta_+\rangle$) or antifringes ($|\eta_-\rangle$).

Now, we proceed with our first strategy for characterizing entanglement in the two-qubit states by measuring in the Schmidt bases. The setup used for this is sketched in Fig. 1(c). Both “pointlike” detectors are in the Fourier transform plane of the double slits. So the detection coincidence rate, which is proportional to $\langle \Psi | \mathbb{E}_s^\dagger \mathbb{E}_i^\dagger \mathbb{E}_i \mathbb{E}_s | \Psi \rangle$, will be given by

$$P_2(x_s, x_i) \propto S^2(x_s) S^2(x_i) \{1 + 2|W_0|^2 \cos[\alpha(x_s - x_i)] + 4|W_0 W_+| \cos(\phi) [\cos(\alpha x_s) + \cos(\alpha x_i)] + 2|W_+|^2 \cos[\alpha(x_s + x_i)]\}, \quad (15)$$

where ϕ is a relative phase between the coefficients W_+ ($=W_-$) and W_0 of Eq. (5) and again $\alpha = kd/2f$ and $S(x) \equiv \text{sinc}(kax/2f)$. The coincidence measurements are made with D_i scanning the x direction at the idler arm, while D_s is kept fixed at (i) $x_s = 0$ and (ii) $x_s = \pi/\alpha$. The results for $|\Psi_1\rangle$, $|\Psi_2\rangle$, and $|\Psi_3\rangle$ are shown in Fig. 3(b) where procedure (i) corresponds to the upper graphs and (ii) to the lower graphs. The interpretation of these results is as follows: in the first case (i), D_s selects *only* signal photons in the state $|\eta_+\rangle_s$ since $P_{\eta_-}(0) = 0$. Thus, the idler photon is projected onto the state $|\eta_+\rangle_i$ and the coincidence counts with the scanning D_i is composed of fringes [see Eq. (15) with $x_s = 0$]. In the second case (ii), D_s selects *only* signal photons $|\eta_-\rangle_s$ because $P_{\eta_+}(\pi/\alpha) = 0$. The idler is projected onto $|\eta_-\rangle_i$ and the coincidence count is composed of antifringes [see Eq. (15) with $x_s = \pi/\alpha$]. So in the first case D_i measures locally (triggered by D_s) the component $|\eta_+\rangle\langle\eta_+|$ and in the second case $|\eta_-\rangle\langle\eta_-|$ of Eq. (10). Since $c_+^2 \in [\frac{1}{2}, 1]$ and $c_-^2 \in [0, \frac{1}{2}]$, observation of the antifringe interference pattern (second component) depends on the degree of entanglement of the overall state as we can see from the graphs of Fig. 3(b). For the sake of normalization we need to measure both patterns with which we compute the probabilities c_{\pm}^2 [17] shown in Fig. 3(c) and then the concurrence for $|\Psi_1\rangle$, $|\Psi_2\rangle$, and $|\Psi_3\rangle$, whose values are shown in Table I (first row). We see there, within the experimental errors, that $|\Psi_1\rangle$ is a maximally entangled state, while $|\Psi_2\rangle$ and $|\Psi_3\rangle$ are only partially entangled. The concurrence errors were great but we can in principle reduce them by increasing the time of measurement

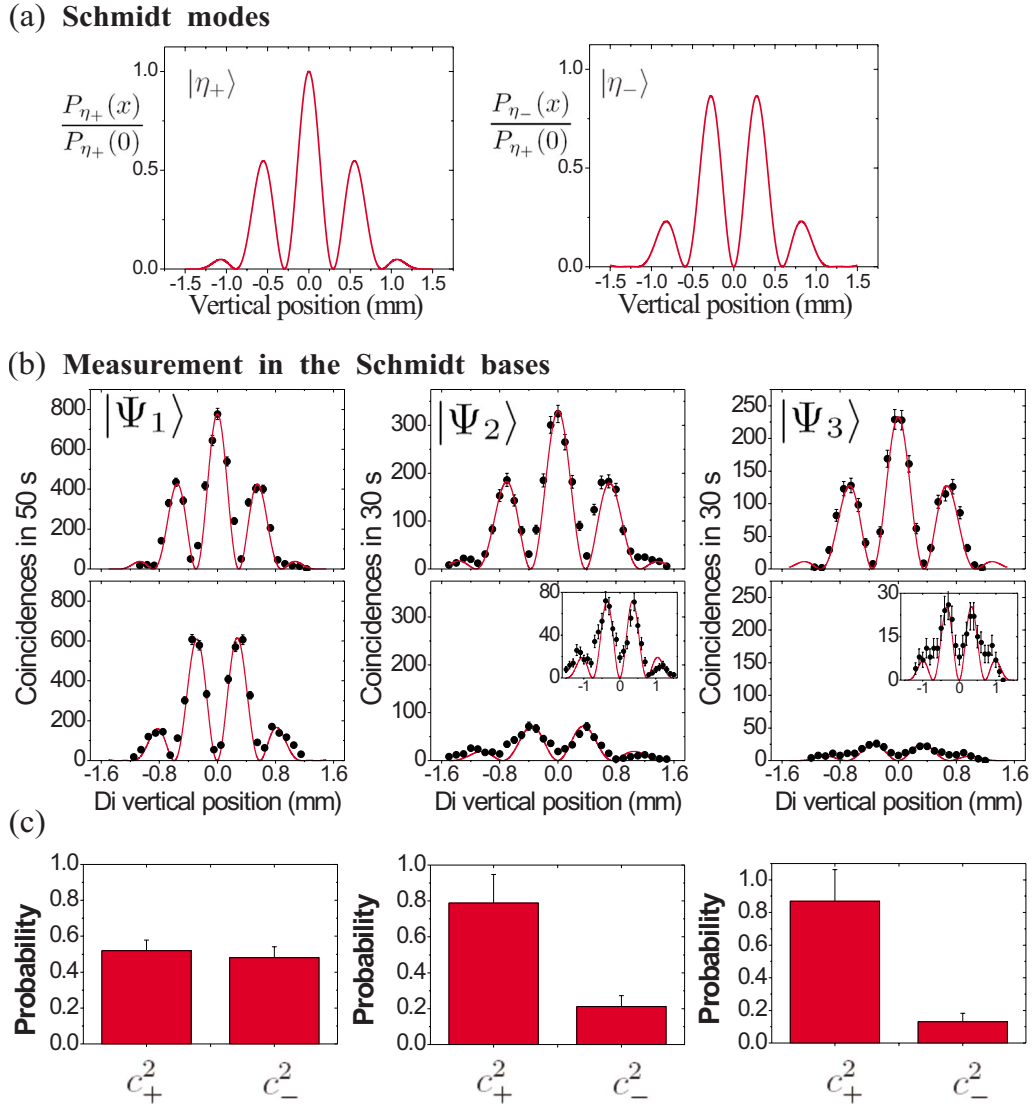


FIG. 3. (Color online) (a) Normalized probability distribution for the Schmidt modes $|\eta_+\rangle$ and $|\eta_-\rangle$. (b) Measurements in the Schmidt bases. Two-photon interference patterns obtained by displacing D_i when D_s is kept fixed at $x_s=0$ mm (upper graphs) and $x_s=(\pi/\alpha)$ mm (lower graphs). The insets show the lower graphs for $|\Psi_2\rangle$ and $|\Psi_3\rangle$ in an adjusted scale. The solid curves were obtained from Eq. (15). (c) Squared Schmidt coefficients.

and/or using more efficient sources. This can be seen for $|\Psi_1\rangle$ in Fig. 3(b), where the greater time of measurement resulted in a smaller error for concurrence.

Physically, we are showing here a direct relation between the degree of entanglement of the spatially entangled qubits and “degree of conditionality” of the interference pattern [18]. The smaller c_-^2 , the smaller the degree of entanglement and also the conditionality of the two-photon interference pattern since the contribution of the second term in Eq. (7)

will be reduced. Besides, observation of almost perfect correlations in two unbiased bases shows that $|\Psi_1\rangle$ is a nearly maximally entangled state and not a classically correlated one, which could be thought if we had just considered the measurements in the basis $\{|\pm\rangle_s \otimes |\pm\rangle_i\}$ shown in the first graphic of Fig. 2(c). Another interesting aspect is that the $|\Psi_3\rangle$ state is not a product state. Although it seems uncorrelated if we look for the measurements in the basis $\{|\pm\rangle_s \otimes |\pm\rangle_i\}$ [third graphic of Fig. 2(c)], there is an unfactorable phase between the coefficients W_0 and W_{\pm} , which have the same modulus, and the measurements in that basis miss it. On the other hand, in the Schmidt decomposition the entanglement is entirely in the real Schmidt coefficients.

D. Measurement of marginal probability

Our second method for determining the amount of entanglement in the prepared states is also local with classical

TABLE I. Concurrence.

	$ \Psi_1\rangle$	$ \Psi_2\rangle$	$ \Psi_3\rangle$
Schmidt	0.99 ± 0.11	0.82 ± 0.20	0.69 ± 0.21
Marg. prob.	0.99 ± 0.01	0.83 ± 0.03	0.72 ± 0.04

communication and also relies on the Schmidt decomposition since we measure in the Fourier transform plane. But now the detector D_s acts in a different way. Rather than select one of the Schmidt modes, it simply registers the presence of the signal photon without registering its position and then triggers a local measurements with the scanning D_i . In this way we are measuring the marginal probability which is the probability $\bar{P}_1(x_i)$ of observing a photon idler (in this case) at x_i and the signal at any location ($-\infty < x_s < +\infty$) [19]. Integrating the coincidence rate in Eq. (15) over the signal detector diameter we obtain

$$\bar{P}_1(x_i) \propto S^2(x_i) \{1 + \sqrt{1 - [\mathcal{C}(\Psi)]^2} \cos(\alpha x_i)\}. \quad (16)$$

Note that although the same expression is obtained just considering the detection on the reduced state (10) [$P_1(x_i) = \text{Tr}(\rho \mathbb{E}^\dagger \mathbb{E})$ with \mathbb{E} given by (13)], which means recording only the single counts at the idler detector regardless of whether the signal is detected or not; here, the triggering is essential because $|\Psi\rangle$ is a post-selected state and we have to be sure that the idler comes from a pair. The important point here is that the visibility of the single-photon marginal interference pattern is directly related to the concurrence, giving us information about the degree of entanglement of the overall state, which is a quite intuitive result: the subsystems of a maximally entangled state are maximally mixed, and then their interference patterns will have null visibilities while at the other extreme, product states have the subsystems in the pure state $|\eta_\pm\rangle$ which gives interference patterns with visibility 1.

The setup configuration for doing these measurements, sketched in Fig. 1(d), is the same as that used for measurements in the Schmidt bases but now the signal detector is totally open (diameter of 12 mm). The experimental marginal interference patterns of such measurements for $|\Psi_1\rangle$, $|\Psi_2\rangle$, and $|\Psi_3\rangle$ are shown in Fig. 4. The visibilities obtained from the theoretical fit using Eq. (16) gave the concurrence for these states. The respective values are shown in the second row of Table I. They are in good agreement with the

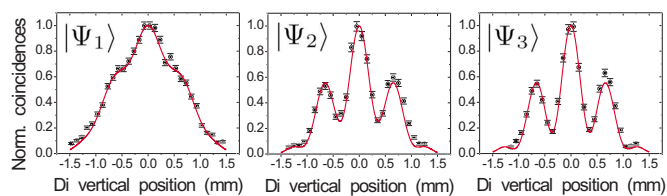


FIG. 4. (Color online) Measurements of the marginal probability. The solid curves were obtained from Eq. (16) with the concurrence as a normalization parameter.

values obtained through the measurement in the Schmidt bases. The smaller errors here are due to the greater signal-to-noise ratio in the measurements of the marginal probability.

IV. CONCLUSION

In summary, we have demonstrated that measurements of either two-photon conditional interference or marginal probabilities can be used for characterizing entanglement in two-qubit pure states created with spatially correlated photons from SPDC. Both strategies are local ones with classical communication, since the photons are detected locally by D_s and D_i while the coincidence triggering correspond to classical communication. Elsewhere, conditional interference was used to distinguish, qualitatively, entanglement from classical correlations for qudits [9,13]. Here we see that such measurements are equivalent to measuring in the Schmidt basis. These results can be easily extended for spatially entangled qudits [8,9]. Therefore, this work introduces a technique for entanglement measurement that can be used for bipartite higher-dimensional spatial-entangled states.

ACKNOWLEDGMENTS

This work was supported by the Brazilian agencies CAPES, FAPEMIG, FAPERJ, CNPq, and the Millennium Institute for Quantum Information.

-
- [1] M. A. Nielsen and I. L. Chuang, *Quantum Computation and Quantum Information* (Cambridge University Press, Cambridge, UK, 2000).
 - [2] W. K. Wootters, Phys. Rev. Lett. **80**, 2245 (1998).
 - [3] U. Leonhardt, *Measuring the Quantum State of Light* (Cambridge University Press, Cambridge, UK, 1997).
 - [4] D. F. V. James, P. G. Kwiat, W. J. Munro, and A. G. White, Phys. Rev. A **64**, 052312 (2001).
 - [5] A. Acín, R. Tarrach, and G. Vidal, Phys. Rev. A **61**, 062307 (2000).
 - [6] J. M. G. Sancho and S. F. Huelga, Phys. Rev. A **61**, 042303 (2000).
 - [7] S. P. Walborn, P. H. Souto Ribeiro, L. Davidovich, F. Mintert, and A. Buchleitner, Nature (London) **440**, 1022 (2006).
 - [8] L. Neves, S. Pádúa, and C. Saavedra, Phys. Rev. A **69**, 042305 (2004).
 - [9] L. Neves, G. Lima, J. G. Aguirre Gómez, C. H. Monken, C. Saavedra, and S. Pádúa, Phys. Rev. Lett. **94**, 100501 (2005); Mod. Phys. Lett. B **20**, 1 (2006).
 - [10] A. Ekert and P. L. Knight, Am. J. Phys. **63**, 415 (1994).
 - [11] C. H. Monken, P. H. Souto Ribeiro, and S. Pádúa, Phys. Rev. A **57**, 3123 (1998).
 - [12] G. Lima, F. A. Torres-Ruiz, L. Neves, A. Delgado, C. Saavedra, and S. Pádúa, e-print arXiv:quant-ph/0703108.
 - [13] G. Lima, L. Neves, I. F. Santos, J. G. Aguirre Gómez, C. Saavedra, and S. Pádúa, Phys. Rev. A **73**, 032340 (2006).
 - [14] The coincidences are measured at the four points of maximum single count of the scanned slit. This number is normalized by the sum of coincidences for all basis states.
 - [15] J. W. Goodman, *Introduction to Fourier Optics* (McGraw-Hill, New York, 1996).

- [16] I. F. Santos, M. A. Sagiuro, C. H. Monken, and S. Pádua, Phys. Rev. A **67**, 033812 (2003).
- [17] Let $n_{+(-)}$ be the number of coincidences in the fringes (anti-fringes) pattern; then, $c_{+(-)}^2 = n_{+(-)} / (n_+ + n_-)$.
- [18] E. J. S. Fonseca, J. C. Machado da Silva, C. H. Monken, and S. Pádua, Phys. Rev. A **61**, 023801 (2000).
- [19] A. F. Abouraddy, B. E. A. Saleh, A. V. Sergienko, and M. C. Teich, Phys. Rev. Lett. **87**, 123602 (2001).